Bull Earthquake Eng (2016) 14:3025–3046
DOI 10.1007/s10518-016-9932-5

ORIGINAL RESEARCH PAPER

Enhanced nonlinear static analysis with the drift pushover procedure for tall buildings

Farhad Behnamfar[1] · Sayed Mehdi Taherian[2] · Arash Sahraei[2]

Received: 25 August 2015 / Accepted: 6 May 2016 / Published online: 14 May 2016

Abstract In this study a new method for nonlinear static analysis based on the relative displacements of stories is proposed that is able to be implemented in a single stage analysis and considers the effects of an arbitrary number of higher modes. The method is called the extended drift pushover analysis procedure (*EDPA*). To define the lateral load pattern, values of the relative displacements of stories are calculated using the elastic modal analysis and the modal combination factors introduced. For determining the combination factors, six different approaches are examined. Buildings evaluated in this study consist of four special steel moment-resisting frames with 10–30 stories. Responses including relative displacements of stories, story shear forces and rotation of plastic hinges in each story are calculated using the proposed approaches in addition to modal pushover analysis and nonlinear dynamic time history analyses. The nonlinear dynamic analysis is implemented using ten consistent earthquake records that have been scaled with regard to *ASCE7-10*. Distribution of response errors of story shears and plastic hinge rotations show that a major part of error corresponds to the second half of the buildings studied. Thus, the mentioned responses are corrected systematically. The final results of this study show that implementing the *EDPA* procedure using the third approach of this research is able to effectively overcome the limitations of both the traditional and the modal pushover analyses methods and predict the seismic demands of tall buildings with good accuracy.

Keywords Drift pushover analysis (*DPA*) · Higher modes · Seismic demands · Tall buildings

✉ Farhad Behnamfar
farhad@cc.iut.ac.ir

[1] Department of Civil Engineering, Isfahan University of Technology, Esfahān 8415683111, Iran

[2] Esfahan, Iran

1 Introduction

The nonlinear static analysis (*NSA*) of structures for seismic evaluation, known also as the pushover analysis method, has been introduced as an affordable substitute for the costly but rigorous nonlinear dynamic analysis. The main components of an *NSA* are the pattern of increasing lateral loads and a maximum (target) displacement for the roof to attain. Introduction of *NSA* goes back to the studies of Gulkan and Sozen (1974). They developed an equivalent nonlinear single-degree-of-freedom (*SDF*) system substituting its associated multi-degree-of-freedom (*MDF*) multi story building. In the same line, simplified nonlinear analysis methods for *MDF* systems were proposed by Saiidi and Sozen (1981) and Fajfar and Fischinger (1988). However, nonlinear analysis was not endorsed by the practice of structural engineering until mid 90's. Release of the documents *ATC-40* (1996) and *FEMA-273* (1997) was a milestone in the process of evolution of engineering analysis with nonlinear static/dynamic methods. A set of nonlinear procedures was also promoted by *SEAOC* in 1995. The conventional pushover analysis method (*CPA*) has its own shortcomings. For instance, Kim and D'Amor implemented a series of comparative analysis with *NSA* and nonlinear dynamic analysis and concluded that use of *NSA* for irregular or tall buildings could result in large errors (Kim and D'Amore 1999). An adaptive pushover method, with the essence of using current dynamic properties of yielding structures for determination of the lateral load pattern, was suggested by Bracci et al. (1997). They reported an increased accuracy in response prediction, compared with that of *CPA*. Antoniou and Pinho introduced a number of alternatives for the adaptive pushover procedure (Antoniou and Pinho 2004), based on story shears and displacements.

Afterwards, efforts were focused on developing multi-modal pushover methods to account for the higher modes and predict the response of taller buildings with acceptable accuracy. Meanwhile, work of Chopra and Goel (2002) succeeded in becoming more widely accepted (Chopra et al. 2004). In their modal pushover analysis (*MPA*), a pushover analysis is implemented each time for a certain mode of vibration and the total nonlinear response is calculated by combination of modal responses. Different alternatives for combination of the adaptive and modal pushover procedures have also been proposed (Gupta and Kunnath 2000; Kalkan and Kunnath 2006). Because *NSA* in essence has been proposed as a simple substitute for the nonlinear dynamic analysis, use of newer versions of *NSA* with increasing complexity might be looked upon as a contradictory move. For the same reason, some researchers have tried to introduce methods that while retain the simplicity of *CPA*, enjoy greater accuracy. In the mentioned methods, use of the adaptive approaches has been refrained from, but the effects of higher modes were taken into account in one way or another. The works of Sahraei and Behnamfar (2014) using the height-wise drift pattern as a basis for NSA, Behnamfar and Tavakoli based on story shears (Tavakoli 2012) and Poursha et al. (2009) introducing a consecutive modal pushover (*CMP*) with use of the mass participation factor for combination of modal responses can be mentioned in this regard.

This paper is an extension of the work of Sahraei and Behnamfar (2014). It aims to extend the pushover analysis to the cases of high-rise buildings while retaining its simplicity. Similar to the mentioned reference again the story drifts are taken to develop the pattern of lateral loads, but in contrast, instead of using the square-root-of-sum-of-the-squares (*SRSS*) procedure to combine the modal drifts, a new combination rule is proposed that retains the sign of the response quantities. Values of the relative displacements of stories are calculated simply using the elastic modal analysis and the theoretical basis of the method is developed utilizing the spectral analysis method. Different approaches are

examined for deriving a combination rule and the modal participation factor. Within various alternatives, the one with more accuracy is explored in detail. Also, a procedure for correction of responses in upper stories is presented. Accuracy of the proposed method is compared with *CPA*, *MPA* and nonlinear time history analysis (*NLTH*), in estimation of story drift, shear and plastic hinge rotations of medium to tall buildings.

2 The extended drift pushover analysis (EDPA)

As mentioned above, the lateral load pattern at the floor levels and the target displacement roof have to be known before implementing a pushover analysis. In the method proposed in this research, new equations are presented for the lateral load pattern but the target displacement is calculated either as the average of the maximum roof displacements under different earthquakes, or as the value determined using the prescribed code-based formula. Therefore, the focus is on the pattern of the lateral load. Value of the lateral displacement of an MDF structure in the j-th mode at the i-th level, u_{ij}, is calculated using Eq. (1) (Chopra 2007):

$$u_{ij} = \Phi_{ij} \cdot y_j \tag{1}$$

in which Φ_{ij} is the i-th component of the j-th column vector of the mode shapes of structure. y_j is the j-th modal response from Eq. (2):

$$y_j = \Gamma_j \cdot S_{dj} \tag{2}$$

where Γ_j and S_{dj} are the j-th mode participation factor and spectral displacement of the j-th mode, respectively, and are determined from Eqs. 3 and 4:

$$\Gamma_j = \frac{L_j}{M_j} \tag{3}$$

$$S_{d_j} = \left(\frac{T_j^2}{4\pi^2}\right) \cdot S_{a_j} \tag{4}$$

In the above equations, L_j, M_j, T_j, and S_{a_j} are the influence factor, modal mass, period, and spectral acceleration of the j-th mode, respectively. L_j and M_j are calculated as:

$$L_j = \phi_j^T \cdot [M] \cdot r \tag{5}$$

$$M_j = \phi_j^T \cdot [M] \cdot \phi_j \tag{6}$$

where ϕ_j is the j-th mode shape column vector, $[M]$ is the mass matrix of structure, and r is the influence column vector with its components being unity for the degrees of freedom in the direction of ground motion, and null elsewhere.

Substitution of Eqs. 2–4 in Eq. 1 results for u_{ij} in:

$$u_{ij} = \Phi_{ij} \cdot \Gamma_j \cdot S_{d_j} = \Phi_{ij} \cdot \Gamma_j \cdot \left(\frac{T^2}{4\pi^2}\right) \cdot S_{a_j} \tag{7}$$

Equation (7) can be rewritten in two different forms:

$$u_{ij} = \bar{u}_{ij} \cdot S_{d_j}, \quad \bar{u}_{ij} = \Phi_{ij} \cdot \Gamma_j \tag{8}$$

$$u_{ij} = \bar{u}_{ij} \cdot S_{a_j}, \quad \bar{u}_{ij} = \Phi_{ij} \cdot \Gamma_j \cdot \left(\frac{T^2}{4\pi^2}\right) \tag{9}$$

The drift at the i-th story in the j-th mode, D_{ij}, can be calculated by deducing the lateral displacement of the roof of the i-th story from that of its floor. This results in:

$$D_{ij} = u_{ij} - u_{i-1j} \tag{10}$$

$$D_{ij} = \Phi_{ij} \cdot \Gamma_j \cdot \left(\frac{T^2}{4\pi^2}\right) \cdot S_{a_j} - \Phi_{i-1j} \cdot \Gamma_j \cdot \left(\frac{T^2}{4\pi^2}\right) \cdot S_{a_j} \tag{11}$$

or:

$$D_{ij} = \bar{\Phi}_{ij} \cdot \Gamma_j \cdot S_{d_j} = \bar{\Phi}_{ij} \cdot \Gamma_j \cdot \left(\frac{T^2}{4\pi^2}\right) \cdot S_{a_j} \tag{12}$$

where:

$$\bar{\Phi}_{ij} = \Phi_{ij} - \Phi_{i-1j} \tag{13}$$

in which $\bar{\Phi}_{ij}$ is rate of change of the *j-th* mode shape in the *i-th* story.

Equation (12) can be re-written in two different forms:

$$D_{ij} = \bar{D}_{ij} \cdot S_{d_j}, \quad \bar{D}_{ij} = \bar{\Phi}_{ij} \cdot \Gamma_j \tag{14}$$

$$D_{ij} = \bar{D}_{ij} \cdot S_{a_j}, \quad \bar{D}_{ij} = \bar{\Phi}_{ij} \cdot \Gamma_j \cdot \left(\frac{T^2}{4\pi^2}\right) \tag{15}$$

The values of the story drifts in each mode, d_{ij}, have to be combined one way or another to account for all of the desired modes. In such a combination, non-concurrency of the maximum modal responses must be considered. A well-known classical method for combining the modal responses is computing the *SRSS* of the modal responses. This method lacks the ability to retain the signs of the responses. In this research keeping the signs of quantities is a prime concern. Then, the question is how to calculate the maximum story drift including: the desired number of modes, accounting for the fact that the maximum drifts do not occur at the same time, and retaining the signs of story drifts in each mode.

Two options are evaluated in this study for tackling the above problem:

1. Direct adding of the modal maximum drifts after modifying each one by a modal participation factor α_{ij} corresponding to the i-th story in the j-th mode. This results in Eq. (16):

$$d_i = \sum_{j=1}^{n} \alpha_{ij}.d_{ij} \tag{16}$$

   in which d_i is the maximum drift of story *i*, and n is the desired number of modes.

2. Direct addition of the modal maximum drifts, and then applying a correction factor to the sum. The correction factor is considered to be the sum of the individual modal participation factors. This approach is illustrated by Eq. 17:

$$d_i = \sum_{j=1}^{n} \alpha_{ij} \cdot \sum_{j=1}^{n} d_{ij} \tag{17}$$

In other words, in the first approach, the responses are first modified and then added, while in the second approach the response are added and then modified.

In addition to how the modal combination is implemented using participation factors, the participation factor itself has also to be introduced. Several options are possible. For each option, the accuracy of results can be evaluated. In this research the following alternative equations have been assessed for accuracy for the modal participation factor:

$$\alpha_{ij} = \left| \frac{\bar{d}_{ij}}{\sum_{j=1}^{n} \bar{d}_{ij}} \right|, \quad \bar{d}_{ij} = \bar{\Phi}_{ij} \cdot \Gamma_j \tag{18}$$

$$\alpha_{ij} = \left| \frac{\bar{d}_{ij}}{\sum_{j=1}^{n} \bar{d}_{ij}} \right|, \quad \bar{d}_{ij} = \bar{\Phi}_{ij} \cdot \Gamma_j \cdot \left(\frac{T^2}{4\pi^2} \right) \tag{19}$$

$$\alpha_{ij} = \left| \frac{\bar{d}_{ij}}{\sqrt{\sum_{j=1}^{n} \bar{d}_{ij}^2}} \right|, \quad \bar{d}_{ij} = \bar{\Phi}_{ij} \cdot \Gamma_j \cdot \left(\frac{T^2}{4\pi^2} \right) \cdot S_{a_j} \tag{20}$$

$$\alpha_j = \left| \frac{\bar{u}_{Nj}}{\sum_{j=1}^{n} \bar{u}_{Nj}} \right|, \quad \bar{u}_{Nj} = \Phi_{Nj} \cdot \Gamma_j \tag{21}$$

$$\alpha_j = \left| \frac{\bar{u}_{Nj}}{\sum_{j=1}^{n} \bar{u}_{Nj}} \right|, \quad \bar{u}_{Nj} = \Phi_{Nj} \cdot \Gamma_j \cdot \left(\frac{T^2}{4\pi^2} \right) \tag{22}$$

$$\alpha_j = \left| \frac{u_{Nj}}{\sqrt{\sum_{j=1}^{n} u_{Nj}^2}} \right|, \quad u_{Nj} = \Phi_{Nj} \cdot \Gamma_j \cdot \left(\frac{T^2}{4\pi^2} \right) \cdot S_{a_j} \tag{23}$$

Equations 18, 19 and 20 are conjoined with Eqs. 14, 15 and 13, respectively. Also, Eqs. 21, 22 and 23 are associated with Eqs. 8, 9 and 7, respectively. In Eqs. 21–23, α_j is the j-th mode participation factor calculated based on the lateral displacement of the roof (N-th story) of building, where N is number of stories. It is used in Eqs. 16 and 17 instead of α_{ij} to calculate the total i-th story drift, d_i. In fact, in Eqs. 18–20, drifts are used as the basis for calculation of α_{ij} while in Eqs. 21–23, lateral displacement of the top story is used for calculating a unique j-th mode participation factor for all stories.

After calculation of α_{ij} or α_j, the story drifts are calculated using Eq. 15 or 16. Then, the load pattern of the equivalent lateral forces, necessary for pushover analysis, is determined from Eq. 24:

$$\bar{f}_i = \frac{u_t}{\sum_{i=1}^{N} d_i} \frac{k_i d_i - k_{i+1} d_{i+1}}{k_1 d_1} \tag{24}$$

In Eq. 24, $\bar{f}_i$ is the load pattern at floor i ($i = 1,\ldots, N$), u_t is the target displacement (at the roof), and k_i is the interstory lateral stiffness of story i. In fact, the first fraction on the

right side of Eq. 24 is meant to correct all story drifts such that their sum, i.e. the lateral displacement at the top of building, equals the known target displacement. The second fraction is simply deduction of the adjacent story shears normalized to the base shear to result in the lateral load pattern.

The EDPA analysis is implemented using Eq. 24 and the prescribed code-based target displacement. The numerical calculations of this research have been employed using four medium to tall buildings (10, 15, 20 and 30 stories) and 10 scaled earthquake records. Responses including lateral displacements, shear forces and absolute sum of plastic hinge rotations in each story have been calculated and compared with the averages of the maximum response values from nonlinear dynamic analysis. In all, about 5000 analysis cases have been implemented (totally 75 stories, 3 response quantities in each story, 10 earthquake records: $75 \times 3 \times 10 = 2250$, 6 different formulas for the participation factor, 2 approaches for modal combination: $75 \times 3 \times 6 \times 2 = 2700$). Out of the above analysis, it was concluded that determining the participation factor using the third approach (Eq. 20) and combining the modal drifts using Eq. 17 results in the most accurate results (Taherian 2014). Because of the huge volume of the analysis, in this paper only the results of the selected method consisting of Eqs. 17 and 20 are presented.

3 The buildings studied

Since the method developed herein is meant to enhance the accuracy of the pushover analysis for taller buildings where the affect of higher modes is more important, a range of stories between 10 and 30 is selected. To cover this interval, four regular residential buildings having 10, 15, 20 and 30 stories are selected. In each building, the structural system consists of special steel moment frames having three bays in each direction. Each bay spans 5 m and the floor to floor story height is uniformly selected to be 3.20 m. The seismicity of the region is assumed to be very high. The ground consists of a medium soil, e.g. soil type C of *NERHP09* (2009). The dead (weight of floors plus partitions) and live loads on the floors are 650 and 200 daN/m^2, respectively, and the diaphragms are rigid.

Before implementing a nonlinear static/dynamic analysis, the structural frames are designed according to AISC-ASD (2010), with the above assumptions. Use is made of I-sections for beams and box sections for columns with the dimensions shown parametrically in Fig. 1 and with specific dimensions in Tables 1 and 2.

Table 3 shows the periods and Fig. 2 exhibits the mode shapes of the first three modes of the designed buildings. It is to be noted that with the use of three modes, at least 90 % of the buildings weight is excited for all the buildings studied.

4 The earthquake records

While use of a minimum of seven earthquake records is enough for when utilizing average of values is targeted, ten strong ground motions are selected for less discrepancy of results. The PEER ground motions database (PEER 2014) is used for selection of earthquake records. The selected records have all been recorded on the soil type C with their magnitudes being in the range of 6–7.5. Table 4 shows the characteristics of the earthquakes selected.

According to *ASCE7-10*, the earthquake records must be scaled before being suitable for time history analysis such that their average spectrum is not lower than the design spectrum in the period range of $0.2T$–$1.5T$ where T is the fundamental period of the

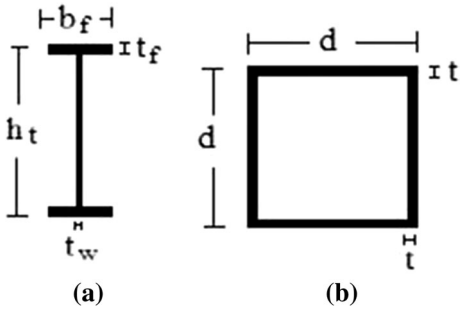

Fig. 1 Cross sections of beams (**a**) and columns (**b**)

Table 1 Types and dimensions of beams and columns

Dimensions of beams	h_t (cm)	t_w (cm)	b_f (cm)	t_f (cm)	Dimensions of columns	d (cm)	t (cm)
B1	50	1	22.5	3	C1	50	3.5
B2	45	1	22.5	2.5	C2	45	3
B3	45	1	22.5	2	C3	40	2.5
B4	40	1	22.5	2	C4	35	2.5
B5	35	0.88	22.5	2	C5	30	2
B6	30	0.8	20	1.5	C6	25	1.5

building under study (see Table 3). Table 5 gives the scale factors for each building-earthquake case. Figure 3 shows the mean spectrum of the 10 records before and after scaling for each building along with the design spectrum.

5 Nonlinear modeling and analysis issues

Modeling of the structures for nonlinear static/dynamic analysis is accomplished in this study using the *OpenSEES* software (Mazzoni et al. 2006). The structures are modeled as plane frames. In *OpenSEES*, the nonlinear behavior of beams and columns of a moment frame can be incorporated either by assuming the plastic deformations all being concentrated at a certain section at the end of the member, or being distributed along the member. While the second approach is obviously more accurate, it is much more common to adopt the first approach, called the concentrated plasticity, for computational efficiency. The same practice is followed in this study. It results in introducing zero-length nonlinear $M-\theta$ springs at both ends of an elsewhere elastic member. The properties of the $M-\theta$ spring are calculated using the resultant moment of axial stresses of the several longitudinal fibers the section is assumed to be composed of. For each steel fiber, a normal stress-normal strain relation must be defined. Several backbone curves are currently available for the steel material in *OpenSEES* to select. Among the possible options, the *Steel02* material has proved to be accurate and efficient enough for nonlinear analysis of plane frames (Mazzoni et al. 2006). This material type is able to follow the gradual elastic–plastic behavior, strain-hardening, the *Bauschinger* effect, and the isotropic/kinematic plastic behavior of steel in cyclic loading/unloading.

The *Steel02* material is used in this study with its properties being as shown in Table 6.

Table 2 Beam and column types of the buildings

Building	Stories	Columns	Beams
10-Story	1–4	C4	B4
	5 and 6	C4	B5
	7 and 8	C5	B5
	9 and 10	C5	B6
15-Story	1–7	C2	B4
	8	C3	B4
	9	C3	B5
	10–12	C4	B5
	13–15	C5	B6
20-Story	1–6	C2	B3
	7–10	C2	B4
	11 and 12	C3 (interior columns)	B4
	11 and 12	C4 (exterior columns)	B4
	13 and 14	C3 (interior columns)	B5
	13 and 14	C4 (exterior columns)	B5
	15	C4	B5
	16 and 17	C5	B5
	18	C5	B6
	19 and 20	C6	B6
30-Story	1–11	C1	B1
	12–14	C1 (interior columns)	B1
	12–14	C2 (exterior columns)	B1
	15–19	C1 (interior columns)	B2
	15–19	C2 (exterior columns)	B2
	20 and 21	C2	B2
	22 and 23	C2	B4
	24 and 25	C2	B5
	26 and 27	C3	B5
	28	C5	B5
	29	C5	B6
	30	C6	B6

Table 3 The first three modal periods of the studied buildings

Building	Periods		
	T_1 (s)	T_2 (s)	T_3 (s)
10-Story	1.699	0.604	0.350
15-Story	2.322	0.852	0.494
20-Story	3.001	1.089	0.643
30-Story	3.771	1.348	0.777

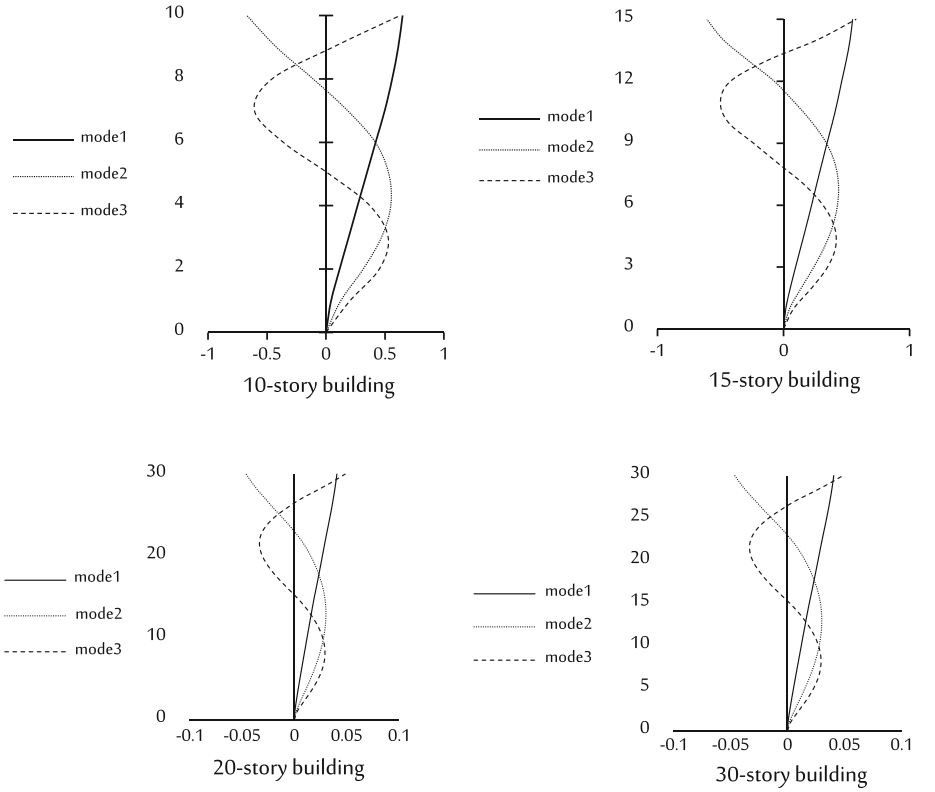

Fig. 2 The first three mode shapes of the buildings under study

Table 4 Characteristics of the selected records

Order	EQ. name	EQ ID	Distance (km)	Magnitude	Year	PGA (g)
1	San Fernando	68	22.8	6.61	1971	0.190
2	Imperial Valley-06	169	22	6.53	1992	0.238
3	Coalinga-01	332	49.4	6.36	1983	0.222
4	Cape Mendocino	826	42	7.01	1992	0.178
5	Landers	900	23.6	7.28	1992	0.241
6	Northridge-01	963	21	6.69	1994	0.457
7	Northridge-01	1086	5.3	6.69	1994	0.840
8	Kobe, Japan	1107	22.5	6.9	1995	0.284
9	Manjil, Iran	1634	75.6	7.37	1990	0.129
10	Hector Mine	1762	43	7.13	1999	0.167

Table 5 Scale factors of the earthquakes

Building	EQ ID									
	68	169	332	826	900	963	1086	1107	1634	1762
10-Story	2.30	1.04	2.72	1.89	1.25	0.67	0.47	1.42	1.43	1.76
15-Story	2.21	1.05	2.71	1.81	1.37	0.93	0.52	1.78	1.38	1.53
20-Story	2.15	1.06	2.75	1.83	1.35	0.93	0.58	1.73	1.57	1.79
30-Story	2.15	1.29	3.29	1.86	1.83	1.01	0.76	2.19	1.51	1.79

6 Numerical results

6.1 Introduction

In this section, results of the nonlinear static/dynamic analysis are presented. The purpose is to see how accurate is the *EDPA* method presented in this research in comparison to the *CPA* and *MPA* methods with regard to the accurate responses determined as the average of maximum responses corresponding to each earthquake. The relative difference of results of the *EDPA*, *CPA* and *MPA* methods with regard to those of the exact nonlinear time-history analysis is calculated using Eq. 25:

$$\mathrm{R.M.S}(\%) = 100\sqrt{\frac{1}{\mathrm{N}}\sum_{\mathrm{i}=1}^{\mathrm{N}}\left(\frac{\mathrm{X_{iD}} - \mathrm{X_{iP}}}{\mathrm{X_{iD}}}\right)^2} \tag{25}$$

in which *RMS* is the error percentage, $\mathrm{X_{iD}}$ the dynamic response calculated at the *i-th* story and X_{iP} is the response at the same story due to the pushover analysis.

6.2 The analysis methods

In the *CPA* method, a certain pattern for distribution of the lateral loads is adopted. Often, this pattern is taken to be proportional to the fundamental mode shape of structure. The lateral loads are increased to the above pattern until the displacement of roof equals a predefined target displacement. At this point, the structural responses are established.

In the *MPA* procedure, a number of lateral load patterns, equal to the number of important modes, are selected. Each load pattern is consistent to the corresponding mode shape of structure. The force–displacement (capacity) curve corresponding to each pattern is drawn. Then the characteristics of the equivalent *SDF* system associated with each mode are calculated using the corresponding capacity curve. Then the target displacement in each mode can be determined. Then the building is pushed in each mode using the modal pattern of lateral loads up to the target displacement of the mode. The desired responses are established in each mode at the target displacement. Finally, the total responses are calculated using a conventional mode combination rule, such as *SRSS*.

In *EDPA*, first the story drifts are calculated using one of the approaches introduced as Eqs. 16–23. Then distribution of lateral forces is calculated using Eq. 24. The structure is pushed upon until the roof displacement becomes equal to the target displacement. The story responses are calculated at this displacement. In the nonlinear time history analysis (*NLTH*), in this study, maxima of lateral displacements and shear forces are calculated at

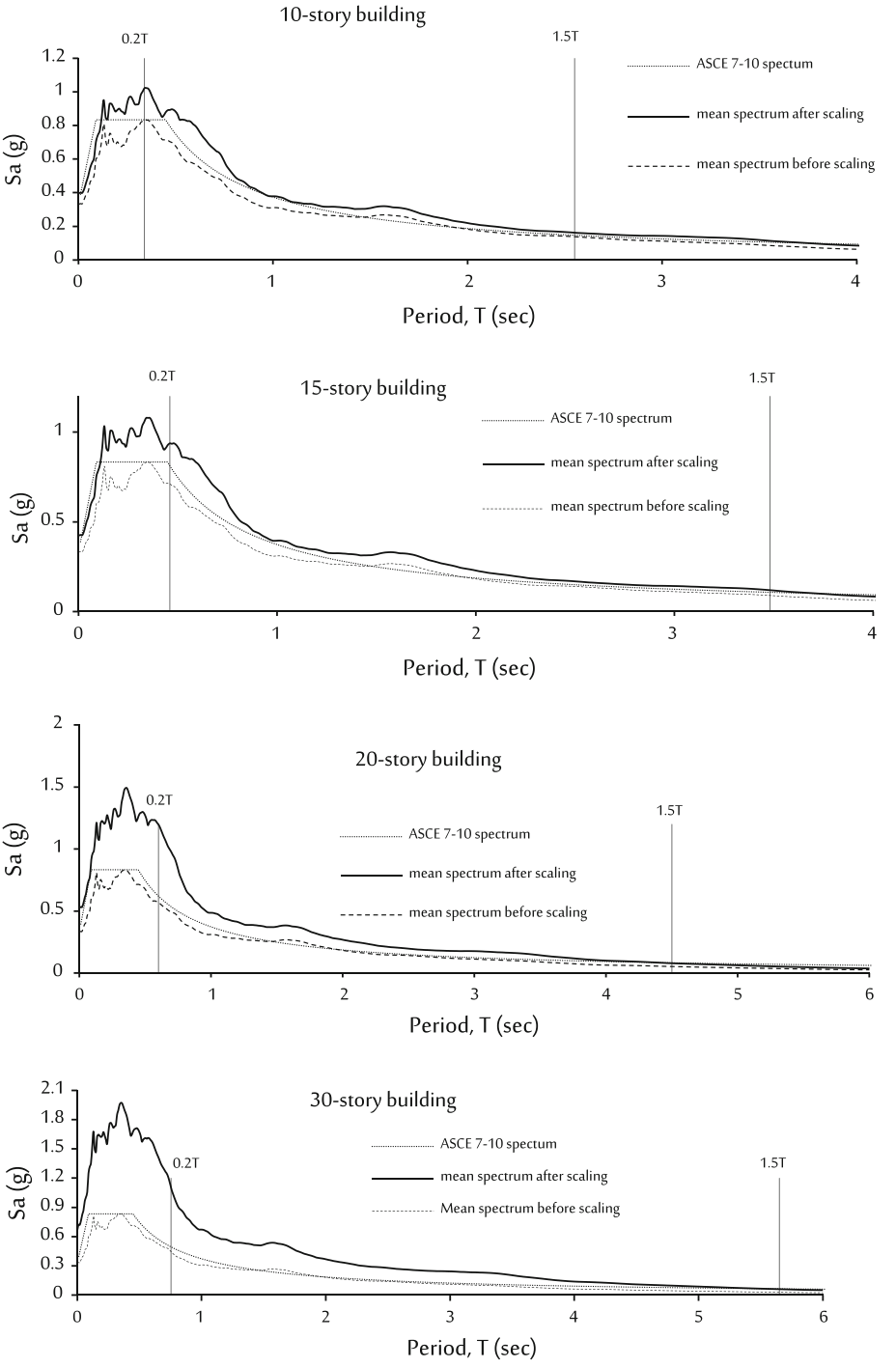

Fig. 3 Mean spectra of the earthquakes before and after scaling

Table 6 Properties of the material Steel02

Parameter	Value
Yield strength (MPa)	235
Young's modulus (MPa)	203,900
Strain-hardening ratio[a]	0.025
Controlling parameter R0[b]	20
Controlling parameter cR1[b]	0.925
Controlling parameter cR2[b]	0.15

[a] The strain-hardening ratio is the ratio between the post-yield stiffness and the initial elastic stiffness

[b] The constants R0, cR1 and cR2 are parameters to control the transition from elastic to plastic branches

each story under each earthquake. Then the averages of the maxima are calculated for the story displacements and shear forces separately and used as a basis of comparison for accuracy analysis of the mentioned pushover procedures. In addition, maxima of the sum of the absolute values of the plastic hinges of beams and columns of each story are processed in the same way as a measure of ductility demand or seismic damage of each story.

6.3 The target displacement

In all of the pushover procedures evaluated in this study, the lateral loads on the buildings are increased up to when the lateral displacement of the roof of each building reaches a predefined value called the target displacement. The target displacement of each building has to be identical for all pushover procedures to make the comparison with the *NLTH* procedure possible. A customary approach is determining the target displacement as being equal to the maximum roof displacement averaged between *NLTH* results under the selected earthquakes. This is not valid for two reasons. First, the pushover analysis is meant to evaluate structures without necessarily resorting to *NLTH* analysis. Then, the maximum roof displacements under earthquakes are not known beforehand in practical cases. Second, taking the maximum displacements from the *NLTH* analysis and then performing the pushover analysis up to such a displacement for comparison with the *NLTH* results inherently makes a prejudice as the pushover analysis will not be independent from *NLTH* procedure in this case. Then, in this research, a more rational approach is adopted with scaling the earthquakes based on a design spectrum and determining the target displacement using the same spectrum. For the latter calculation, the method of displacement coefficient of *ASCE41-13* is followed [21]. The target displacements of the buildings under study are calculated to be 24.60, 33.28, 44.17 and 55.19 cm for 10, 15, 20 and 30-story buildings, respectively.

6.4 The analysis results

6.4.1 Modal participation factors and lateral load patterns

The modal participation factor,α_{ij}, is calculated using Eq. (20). The results are mentioned in Table 7 for each mode and collectively for each story of the buildings under study. As seen, values of α_{ij} in the first mode are larger at the lower floors than those of the top floors.

Table 7 Values of α_{ij}

Story number	α_{i1}				α_{i2}				α_{i3}				$\sum \alpha_{ij}$			
	10	15	20	30	10	15	20	30	10	15	20	30	10	15	20	30
1	0.91	0.98	0.98	0.85	0.37	0.17	0.17	0.46	0.16	0.06	0.06	0.26	1.45	1.22	1.22	1.57
2	0.93	0.98	0.98	0.85	0.34	0.17	0.17	0.46	0.12	0.06	0.06	0.25	1.39	1.21	1.21	1.56
3	0.96	0.99	0.99	0.87	0.27	0.16	0.16	0.44	0.03	0.05	0.05	0.23	1.27	1.19	1.19	1.54
4	0.99	0.99	0.99	0.88	0.14	0.15	0.15	0.43	0.07	0.04	0.04	0.21	1.21	1.17	1.17	1.51
5	0.99	0.99	0.99	0.90	0.03	0.13	0.13	0.40	0.16	0.02	0.02	0.17	1.18	1.14	1.14	1.47
6	0.96	0.99	0.99	0.92	0.20	0.10	0.10	0.38	0.18	0.00	0.00	0.13	1.34	1.10	1.10	1.43
7	0.92	1.00	1.00	0.94	0.39	0.08	0.08	0.34	0.11	0.01	0.01	0.09	1.41	1.09	1.09	1.36
8	0.84	1.00	1.00	0.95	0.54	0.05	0.05	0.30	0.07	0.03	0.03	0.04	1.45	1.08	1.08	1.29
9	0.74	1.00	1.00	0.97	0.62	0.02	0.02	0.26	0.27	0.04	0.04	0.02	1.63	1.06	1.06	1.24
10	0.67	1.00	1.00	0.98	0.63	0.01	0.01	0.21	0.38	0.06	0.06	0.07	1.69	1.07	1.07	1.26
11	–	1.00	1.00	0.98	–	0.05	0.05	0.15	–	0.06	0.06	0.12	–	1.11	1.11	1.26
12	–	0.99	0.99	0.98	–	0.10	0.10	0.10	–	0.06	0.06	0.17	–	1.16	1.16	1.25
13	–	0.99	0.99	0.98	–	0.15	0.15	0.03	–	0.05	0.05	0.21	–	1.19	1.19	1.22
14	–	0.98	0.98	0.97	–	0.19	0.19	0.04	–	0.03	0.03	0.24	–	1.20	1.20	1.25
15	–	0.97	0.97	0.96	–	0.23	0.23	0.10	–	0.01	0.01	0.27	–	1.21	1.21	1.32
16	–	–	0.96	0.95	–	–	0.27	0.16	–	–	0.03	0.27	–	–	1.26	1.38
17	–	–	0.95	0.94	–	–	0.31	0.22	–	–	0.08	0.27	–	–	1.33	1.43
18	–	–	0.93	0.93	–	–	0.34	0.28	–	–	0.13	0.24	–	–	1.40	1.45
19	–	–	0.92	0.92	–	–	0.36	0.34	–	–	0.17	0.21	–	–	1.45	1.46
20	–	–	0.92	0.90	–	–	0.35	0.40	–	–	–	0.16	–	–	–	1.46
21	–	–	–	0.88	–	–	–	0.46	–	–	–	0.09	–	–	–	1.43
22	–	–	–	0.86	–	–	–	0.51	–	–	–	0.00	–	–	–	1.37
23	–	–	–	0.83	–	–	–	0.56	–	–	–	0.08	–	–	–	1.47
24	–	–	–	0.79	–	–	–	0.59	–	–	–	0.17	–	–	–	1.55

Table 7 continued

Story number	α_{i1}				α_{i2}				α_{i3}				$\sum \alpha_{ij}$			
	10	15	20	30	10	15	20	30	10	15	20	30	10	15	20	30
25	–	–	–	0.76	–	–	–	0.61	–	–	–	0.24	–	–	–	1.60
26	–	–	–	0.72	–	–	–	0.61	–	–	–	0.31	–	–	–	1.65
27	–	–	–	0.70	–	–	–	0.61	–	–	–	0.37	–	–	–	1.68
28	–	–	–	0.66	–	–	–	0.61	–	–	–	0.44	–	–	–	1.71
29	–	–	–	0.65	–	–	–	0.59	–	–	–	0.47	–	–	–	1.72
30	–	–	–	0.65	–	–	–	0.58	–	–	–	0.49	–	–	–	1.72

In the higher modes a reverse trend is observed. Also, α_{ij} generally decreases with the mode number.

For all the buildings studied, $\sum_{j=1}^{n} \alpha_{ij}$ varies between 1 and 2, and its variation along height (changing i) for a certain building is smooth. The maximum variation of $\sum_{j=1}^{n} \alpha_{ij}$ as the relative difference between its minimum and maximum value for a specific building, is observed to be about 30 %.

The distribution of lateral forces corresponding to the utilized pushover methods is shown in Fig. 4.

In Fig. 4, distribution of lateral story forces in *CPA* is proportional to the fundamental mode shape of each building. In *MPA*, the distribution is consistent with the mode shape (multiplied by distribution of structural mass) of each mode. In the figure, this distribution is given for the first three modes. In *EDPA*, the distribution is calculated with Eq. 24. Therefore, in *EDPA* contrary to *MPA*, a combination of modal drifts is used to determine the distribution instead of each individual mode. In the figure, number of modes is three for *EDPA*. According to Fig. 4, distribution of lateral forces in *EDPA* is similar to the first mode in the lower stories. For taller buildings, the lateral distribution in *EDPA* distorts in the higher stories due to larger participation of the higher modes.

6.4.2 *Lateral displacements*

Figure 5 shows distribution of lateral displacements of stories for the *CPA*, *MPA* and *EDPA* procedures along with the averaged maxima of the *NLTH* analysis method. The RMS's of errors with regard to the *NLTH* results are mentioned in Table 8.

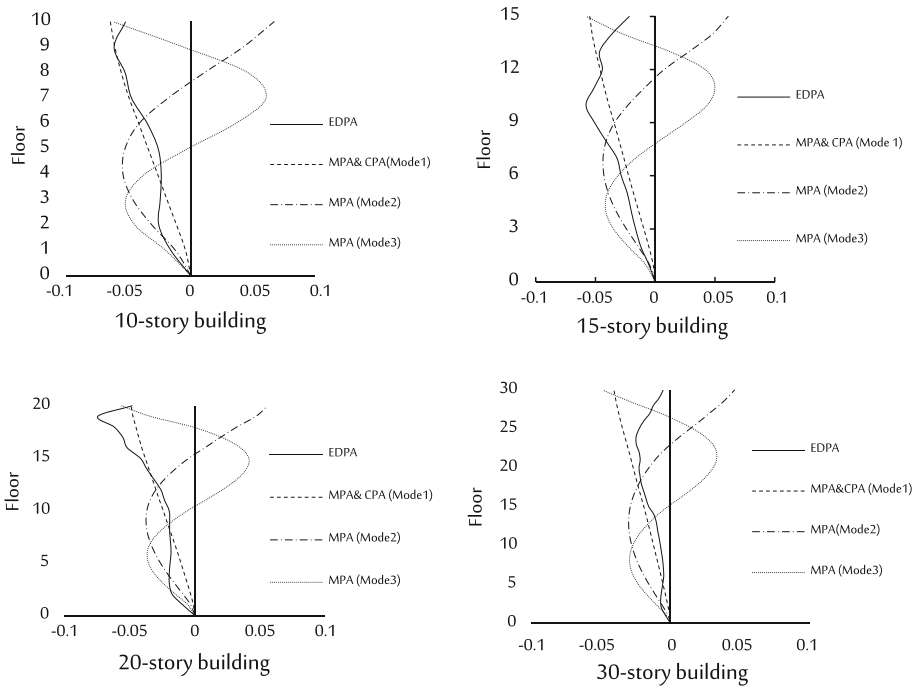

Fig. 4 Distribution of lateral loads in pushover analyses

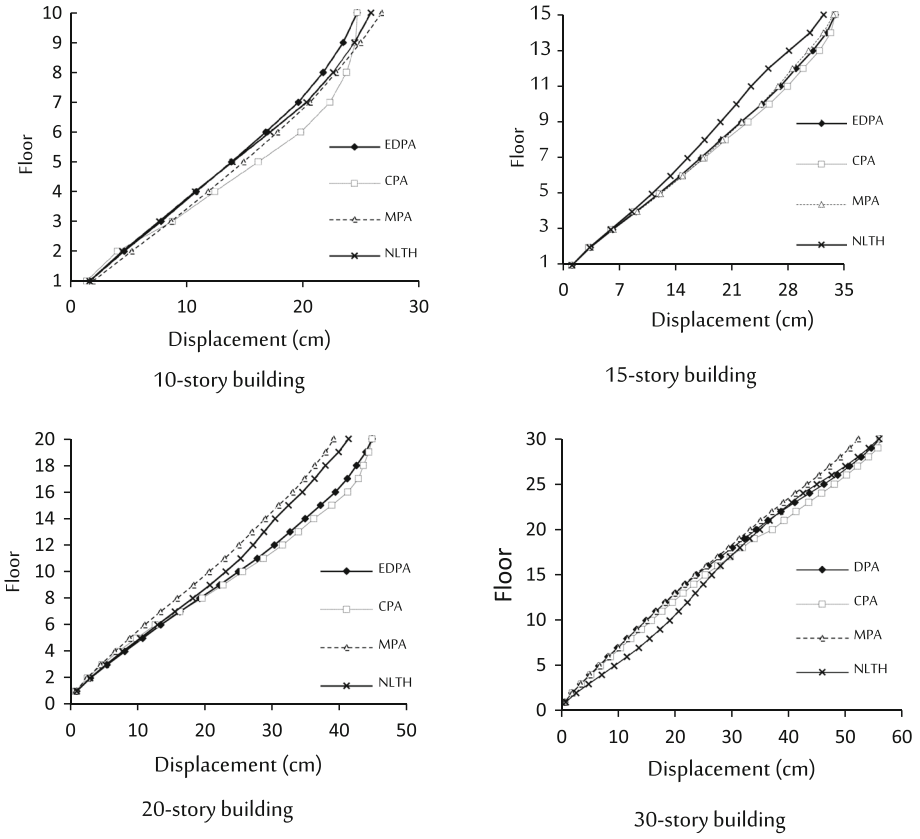

Fig. 5 Lateral displacements of stories

According to Fig. 5, prediction of displacements is generally good in all of the pushover procedure studied. In most cases, error is larger in the upper half of a building. As observed in Table 8, while the *RMS* value of *MPA* is less than *CPA* in all cases, the smallest *RMS* in all buildings belongs to *EDPA*. Therefore, *EDPA* has been successful to predict the maximum floor displacements of the studied buildings with a better accuracy with regard to the other pushover methods. While the displacement prediction error increases among the above pushover method for the taller buildings, it remains below 17 % for *EDPA* and *MPA* but reaches 19 % for *CPA*.

6.4.3 Story shear forces

Figure 6 illustrates the story shears using the above analysis methods. Also, Table 9 gathers the *RMS* errors of the pushover methods in estimation of the story shears. The overall error in prediction of story shears in all of the above pushover methods has been increased relative to displacement predictions. At the same time, *EDPA* possesses the smallest shear *RMS* errors between the others, being at most 29 % for the 20-story building. *MPA* comes next with 30 % and the largest error belongs to *CPA*, which is 35 %.

Table 8 *RMS* errors of pushover displacements with regard to those of the *NLTH* analysis

Building	Method		
	EDPA	CPA	MPA
10-Story	2.94	12.65	10.20
15-Story	9.64	13.45	10.45
20-Story	9.34	13.34	10.20
30-Story	16.67	18.53	16.61

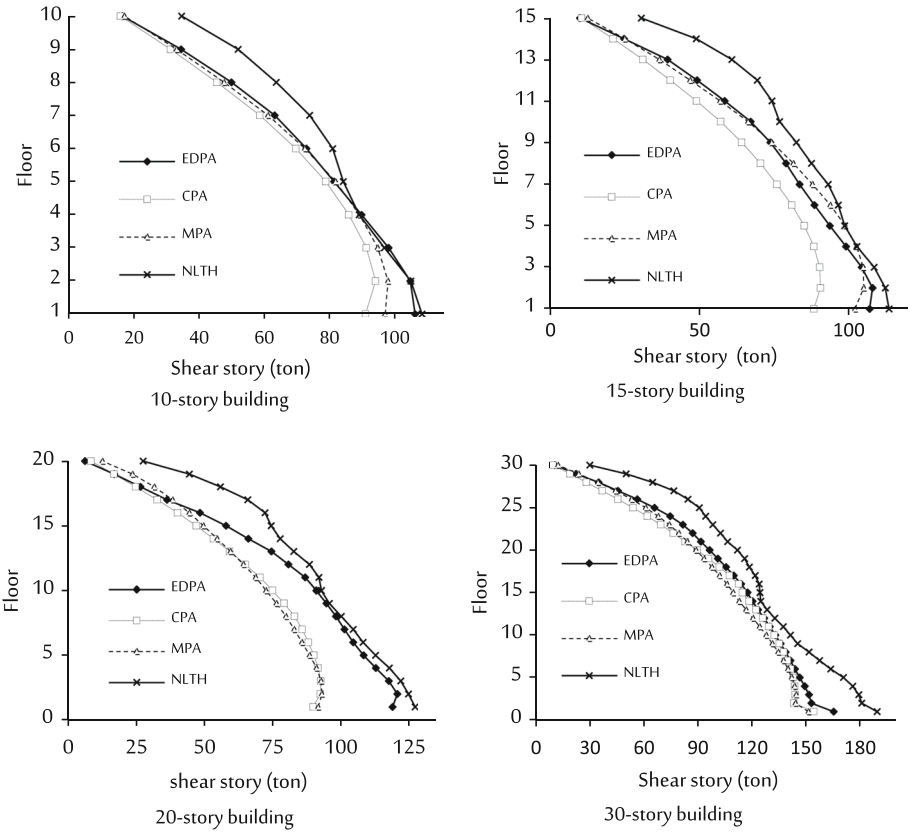

Fig. 6 Total shear forces of stories

EDPA is most successful in the lower half stories. It tends to an error similar to other methods in the upper stories.

6.4.4 Plastic hinge rotations

The sum of the absolute values of the plastic hinge rotation in all plastic hinges of the beams and columns of each story, called the story plastic hinge rotation, are calculated in this section. The ability of each pushover method to predict these values is quantified with

Table 9 *RMS* errors of story shear forces relative to the NLTH responses

Building	Method		
	EDPA	CPA	MPA
10-Story	21.55	25.22	23.39
15-Story	25.90	26.60	25.10
20-Story	28.83	34.40	29.79
30-Story	23.30	28.84	25.53

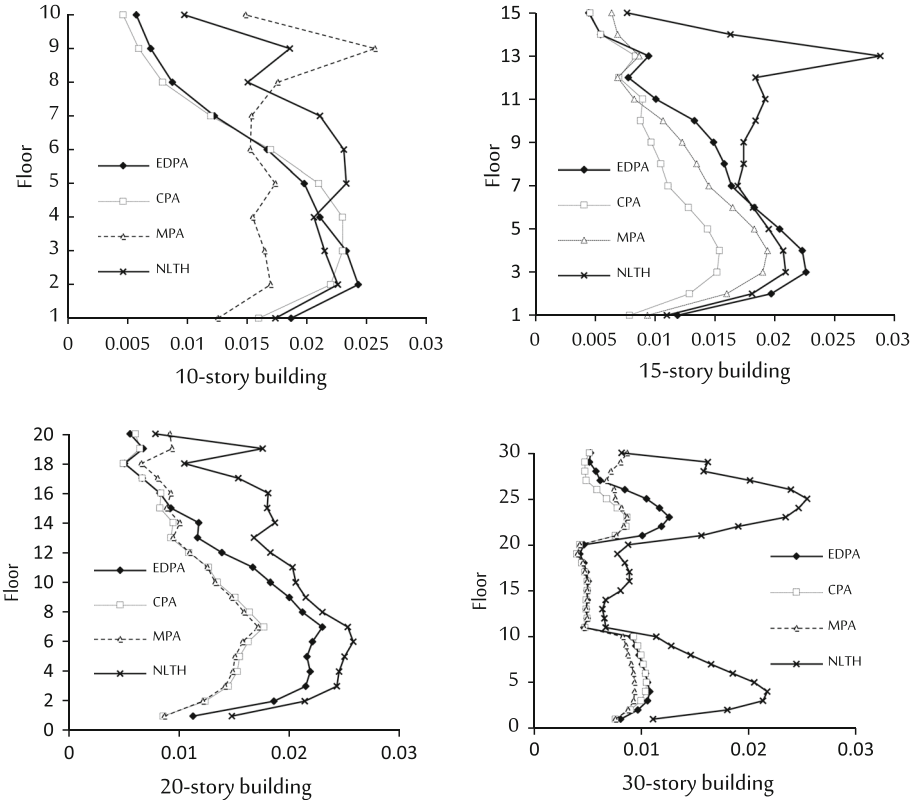

Fig. 7 Total plastic hinge rotations of stories

its *RMS* error with regard to *NLTH* response. Figure 7 shows the story plastic hinge rotations. The *RMS* values of errors of the pushover methods are mentioned in Table 10.

Figure 7 shows that generally *EDPA* has been successful in prediction of plastic hinge rotations with good accuracy in the lower half of structures (perhaps except of the 30-story building). The prevailing trend is that the prediction errors reach to their largest values for plastic hinge rotations compared to shear forces and displacements. The error is larger for taller buildings. Meanwhile, the largest error belongs again to *CPA* with 55 %; next is *MPA* with 48 %, and the least value belongs to *EDPA* with 45 %.

Table 10 RMS errors of story plastic hinge rotations relative to the NLTH responses

Building	Method		
	EDPA	CPA	MPA
10-Story	31.25	35.24	30.75
15-Story	34.07	43.99	35.96
20-Story	31.92	42.11	39.16
30-Story	44.54	49.81	48.13

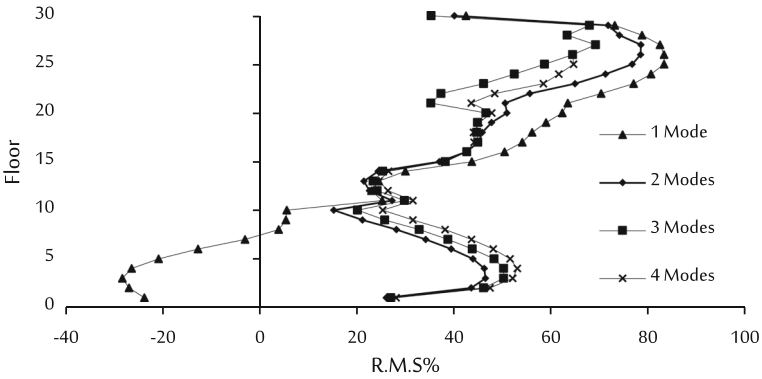

Fig. 8 Story hinge rotations as predicted by EDPA including different numbers of modes

6.4.4.1 Enhancing accuracy of EDPA While in prediction of the nonlinear maximum seismic responses of the tall buildings studied, *EDPA* has been marginally more successful than *MPA*, it is much easier to implement because it is accomplished only in one stage. This is in contrast to *MPA* that must be repeated for all of the important modes.

Number of modes necessary to be included in *EDPA* is simply number of modes with a total effective modal mass of at least 90 % of the seismic mass of building. For all of the studied structures the above criterion results in inclusion of only 3 modes. To evaluate the accuracy, the story hinge rotations of the 30-story building are illustrated in Fig. 8 using 1, 2, 3 and 4 modes for comparison. This figure and other figures alike for other responses and other buildings confirms the above criterion that only modes with a total relative effective mass of over 90 % are enough for the *EDPA* procedure.

On the other hand, if distribution of *RMS* errors along height of each building is investigated, a correction for *EDPA* can be derived that results in a considerably enhanced accuracy for this method.

Table 11 shows the values of *EDPA*'s *RMS* errors for different responses of each building averaged between the lower and upper half stories separately. It shows that *EDPA* is much less successful in estimation of shear and hinge rotations of the upper stories than it is in the lower ones.

Because the average error in estimation of displacement is small it is not discussed further.

Table 12 mentions the average correction factors that if are multiplied by the corresponding responses of the upper half stories, will result in accurate average values of *NLTH*.

The correction factors of Table 12 all happen to be placed between 1 and 2. Moreover, they are very similar to $\sum_{j=1}^{n} \alpha_{ij}$ values of the upper half stories mentioned in Table 7.

Table 11 Average of RMS errors of EDPA in the lower and upper half stories

Building	Average *RMS* error					
	Displacement		Shear		Plastic hinge rotation	
	Lower half	Upper half	Lower half	Upper half	Lower half	Upper half
10-Story	6.98	1.3	2.24	26.05	11.73	38.81
15-Story	−1.34	−6.44	3.59	27.72	5.86	44.22
20-Story	4.85	−2.71	7.36	35.63	11.55	44.89
30-Story	4.49	−9.19	14.7	30.45	34.97	49.99

Table 12 Correction factors of average EDPA responses in the upper half stories to be resembled to those of NLTH

Building	Correction factor for average story shear	Correction factor for average plastic hinge rotation
10-Story	1.35	1.63
15-Story	1.38	1.79
20-Story	1.55	1.81
30-Story	1.44	1.99

Table 13 RMS errors of EDPA with/without correction and other procedures relative to NLTH

Building	Method					
	Story shear			Plastic hinge rotation		
	EDPA		MPA	EDPA		MPA
	With correction	Without correction		With correction	Without correction	
10-Story	11.22	21.55	23.39	12.87	31.25	30.75
15-Story	14.52	25.90	25.10	22.38	34.07	35.96
20-Story	20.52	28.83	29.79	22.92	31.92	39.16
30-Story	17.60	23.30	25.53	32.75	44.54	48.13

Therefore, while it is possible to derive regression equations for correction factors of responses of the upper half stories, it is easier and more consistent to assign $\sum_{j=1}^{n} \alpha_{ij}$ as the response correction factors as follows:

$$\bar{X}_i = \begin{cases} X_i & \text{if } i < \left[\frac{N}{2}\right] \\ X_i \cdot \sum_{j=1}^{N} \alpha_{ij} & \text{if } i \geq \left[\frac{N}{2}\right] \end{cases} \quad (26)$$

in which […] shows the integer part, X_i is the uncorrected shear or plastic hinge rotation of story i, and $\bar{X}_i$ is the associated corrected value.

To evaluate the above correction procedure, the *RMS* errors are again calculated for the studied buildings but this time with *EDPA* with correction. The results are mentioned in Table 13 in comparison to those of *MPA* and *EDPA* without correction. As observed, when corrected, the accuracy of *EDPA* will be much superior to *MPA* and is located within the acceptable margin of error for design applications.

7 Conclusions

In this study a drift based pushover for estimation of nonlinear seismic responses of structures was presented. The theory of the method was derived using the basics of the spectral analysis method using story drifts. Spectral drifts in each mode were combined to calculate the total story drifts and the distribution of lateral forces for pushover analysis. With adhering to the condition of preserving the signs of response values, two different approaches for a combination rule and six various equations for the modal participation factor were examined. The procedure with the least errors was explored in detail. The selected procedure was superior in accuracy and easier in implementation compared with the existing well-known pushover methods. Finally, the sum of the modal participation factors in each story was used as a correction factor for maximum story shears and plastic hinge rotations. It enhanced the accuracy of the proposed method to a level much superior to other available pushover methods.

References

American Institute of Steel Construction (2010) Manual of steel construction, allowable stress design. AISC-ASD, Chicago, IL

Antoniou S, Pinho R (2004) Advantages and limitations of adaptive and non-adaptive force-based pushover procedure. J Earthquake Eng 8:497–522. doi:10.1142/S1363246904001511

Applied Technology Council (1996) Seismic evaluation and retrofit of concrete buildings. Report. ATC-40, Redwood City

Applied Technology Council 1997. NEHRP Guide lines for the seismic rehabilitation of buildings. FEMA-273

Applied Technology Council (2009) NEHRP (National Earthquake Hazards Reduction Program). Recommended seismic provisions for new buildings and other structures (FEMA P-750). Federal Emergency Management Agency, Washington, DC

Bracci J, Kunnath S, Reinhorn A (1997) Seismic performance and retrofit evaluation of reinforced concrete structures. J Struct Eng 123:3–10. doi:10.1061/(ASCE)0733-9445(1997)

Chopra AK (2007) Dynamics of structures, theory and applications to earthquake engineering, 3rd edn. Prentice Hall, Upper Saddle River

Chopra A, Goel R (2002) A modal pushover analysis procedure for estimating seismic demands for buildings. Earthquake Eng Struct Dynam 31:561–582. doi:10.1002/eqe.144

Chopra A, Goel R, Chintanapakdee C (2004) Evaluation of a modified MPA procedure assuming higher modes as elastic to estimate seismic demands. Earthq Spectra 20:757–778. doi:10.1193/1.1775237

Fajfar P, Fischinger M (1988) N2-A method for nonlinear seismic analysis of regular buildings. In: Proceeding of the 9th WCEE, Tokyo-Kyoto, Japan, pp 111–116

Gulkan P, Sozen M (1974) Inelastic response of reinforced concrete structures to earthquake motions. ACI J 71:604–610

Gupta B, Kunnath SK (2000) Adaptive spectra-based pushover procedure for seismic evaluation of structures. Earthq Spectra 16:367–391

Kalkan E, Kunnath SK (2006) Adaptive modal combination procedure for nonlinear static analysis of building structures. J Struct Eng ASCE 132:1721–1731

Kim S, D'Amore E (1999) Pushover analysis procedures in earthquake engineering. Earthq Spectra 15:417–434

Mazzoni S, McKenna F, Scott M, Fenves G, Jeremic B (2006) Opensees command language manual. Pacific Earthquake Engineering Research Center (PEER), University of California, Berkeley, California

Pacific Earthquake Engineering Research Center (2011) PEER ground motion database. http://peer.berkeley.edu/peergroundmotiondatabase/site

Poursha M, Khoshnoudian F, Moghadam AS (2009) A consecutive modal pushover procedure for estimating the seismic demands of tall buildings. Eng Struct 31:591–599

Sahraei A, Behnamfar F (2014) A drift pushover analysis procedure for estimating the seismic demands of buildings. Earthq Spectra 30:1601–1618

Saiidi M, Sozen M (1981) Inelastic response of reinforced concrete structures to earthquake motions. J Struct Div ASCE 10(ST5):937–952

Taherian SM (2014) The drift pushover analysis procedure based on the relative displacement of stories for seismic evaluation of structures. Master thesis, Islamic Azad University, Esfahan, Science and Research Branch

Tavakoli BG (2012) Nonlinear static analysis based on story shear forces. Master thesis, Islamic Azad University, Najaf Abad Branch

Vision 2000, SEAOC (1995) Performance based seismic engineering of buildings. Structural Engineers Association of California, Sacramento, California